Inter-tetrahedra bond angle of permanently densified silicas extracted from their Raman spectra

2010 J. Phys.: Condens. Matter 22 025401

(http://iopscience.iop.org/0953-8984/22/2/025401)

J. Phys.: Condens. Matter **22** (2010) 025401 (6pp) doi:10.1088/0953-8984/22/2/025401

Inter-tetrahedra bond angle of permanently densified silicas extracted from their Raman spectra

B Hehlen

Laboratoire des Colloïdes, Verres et Nanomatériaux, UMR 5587 CNRS and University of Montpellier II, F-34095 Montpellier, France

E-mail: bernard.hehlen@univ-montp2.fr

Received 9 October 2009, in final form 16 November 2009
Published 9 December 2009
Online at stacks.iop.org/JPhysCM/22/025401

Abstract

Relative Raman scattering intensities are obtained in three samples of vitreous silica of increasing density. The variation of the intensity upon densification is very different for bending and stretching modes. For the former we find a Raman coupling-to-light coefficient $C_B \propto \omega^2$. A comparative intensity and frequency dependence of the Raman spectral lines in the three glasses is performed. Provided the Raman spectra are normalized by C_B, there exists a simple relation between the Si–O–Si bond angle and the frequency of all O-bending motions, including those of fourfold ($n = 4$) and threefold ($n = 3$) rings. For 20% densification we find a reduction of $\sim$5.7° of the maximum of the network angle distribution, a value in very close agreement with previous NMR experiments. The threefold and fourfold rings are weakly perturbed by the densification, with a bond angle reduction of $\sim$0.5° for the former.

1. Introduction

There exists two different ways to describe the structure of vitreous silica (v-SiO_2). The first one considers well-defined SiO_4 tetrahedra connected to each others by oxygen atoms. Within this picture, it is the large angular spread of the oxygen 'kneecap' bonds between adjacent tetrahedra that creates the disorder at larger length scales [1, 2]. The second conventional structural description of silica considers a random network of loose Si–O–Si bonds [3]. At larger scale, the elementary structural units (i.e. the SiO_4 tetrahedra or the Si–O–Si bonds) form non-planar $(Si–O–Si)_n$ rings with a large n distribution. These define the medium range order of v-SiO_2. Numerical simulations have shown that the most probable ring size is for $n = 6$ [4]. This relatively open structure leads to a free volume fraction greater in silica than in other network glasses, such as GeO_2 [5]. It is the reason why v-SiO_2 can densify up to $\sim$20% without significant coordination change of the Si atoms, nor deformation of the SiO_4 tetrahedra [6, 7]. Upon compression the ring structure puckers and the elastic-to-plastic limit probably occurs for pressures that produce new bondings in the glass. When the pressure is released from above this limit, the high pressure structure is partially retained. Up to 20% densification, the permanently densified silicas (d-SiO_2) are mostly characterized by a smaller Si–O–Si angle and a probable redistribution of some oxygen bonds. These structural modifications translate into the Raman spectra by frequency shifts and line broadenings (or narrowings) of the vibrational bands. For example, the frequency increase of the R, D_1 and D_2 spectral lines upon densification is attributed to the reduction of the Si–O–Si angle [3]. All of these Raman vibrations involve oxygen-atom displacements along the Si–O–Si bisector in the plane of the structural unit (the so-called below O-*bending* vibrations). The latter sometimes defines the bending axis in the numerical simulations. D_1 and D_2 are called 'breathing modes', as they correspond to in-phase O-bending motion in fourfold ($n = 4$) and threefold ($n = 3$) rings, respectively [8], without significant displacement of the Si atoms [9, 10]. The vibrations leading to the R-band involve a weak contribution from the two adjacent silicon atoms of the Si–O–Si bond, in addition to the O-bending one [11]. These modes are probably closer to pure bendings.

Although many investigations performed in d-SiO_2 report on structural modifications shown by Raman scattering, very few of these have been related to quantitative estimates. In addition, the measurement of the relative intensities from a set of glasses is usually not easily accessible and has only been little exploited [12]. However, such experimental

characterizations are of interest in particular because the local and medium range structure of d-SiO_2 likely depends on the densification cycle, and numerical simulation results should thus be considered cautiously. Combining time-resolved and standard Raman scattering, we recently accessed the concentration of small rings in d-SiO_2. For 20% densification, we found an increase by a factor of ∼4 of the threefold rings while it is only ∼1.5 for the fourfold ones [5]. In the present report, we will show that the Raman coupling coefficient of the O-bending vibrations qualitatively agrees with the prediction of simulations [13]. Combining these results with the simple nearest-neighbor central-force model description developed earlier [3], it is possible to quantitatively estimate the Si–O–Si bond angle in the network and in the small rings. The laboratory-scale analysis developed below could become a standard characterization method of densified glasses (mechanically or neutron irradiated), hydrated silicas and silica-based glasses of industrial or geological interest. The two densified silica samples of density $\rho = 2.43$ and 2.63 g cm^{-3}, and the normal silica glass, with $\rho = 2.21$ g cm^{-3} are described in [5] together with the experimental Raman set-up. We only recall here that special attention was paid during the densification process in order to reduce the glass-density fluctuations at micrometer scales. A value $\Delta\rho/\rho \leqslant 1\%$ was measured by high resolution Brillouin scattering experiments in the two densified glasses. In addition, the utmost care was taken to measure the relative Raman intensities between the three glasses. A crossed analysis of our data with those obtained using femtosecond impulsive-stimulated Raman scattering supports the reliability of our intensity measurements [5].

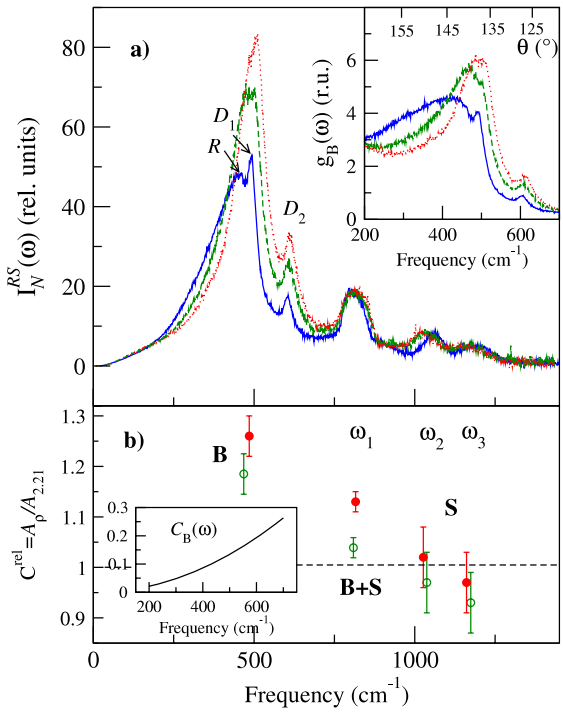

Figure 1. (a) Normalized Raman reduced VV spectra in silicas. '——' $\rho = 2.21$ g cm^{-3} (blue), '- - - -' $\rho = 2.43$ g cm^{-3} (green) and '· · · · · ·' $\rho = 2.63$ g cm^{-3} (red). The inset shows the density of states $g_B(\omega)$ of the Raman-active O-bending vibrations. (b) Areas of the R-, ω_1-, ω_2-and ω_3-spectral lines in d-SiO_2 relative to that in v-SiO_2, $C^{rel} = \mathcal{A}(\rho)/\mathcal{A}(2.21)$: '○' $\rho = 2.43$ g cm^{-3} (green) and '●' $\rho = 2.63$ g cm^{-3} (red). It is the Raman coupling coefficient of the Si–O–Si bending modes which is the most affected by the densification. Inset: frequency dependence of the Raman coupling coefficient of the O-bending modes, $C_B(\omega)$.

(This figure is in colour only in the electronic version)

2. Normalized Raman intensities

In a first-order Stokes Raman process, an incident photon of frequency ω_I scatters a photon of frequency ω_S after interaction with a vibrational excitation σ of frequency $\omega_\sigma = \omega_S - \omega_I$ in the media. For molecular vibrations, the Raman scattering cross section of a probed volume V_S is given by [14]

$$I^{RS}(\omega_\sigma) = \frac{\hbar\omega_I\omega_S^3 V_S}{2c^4\omega_\sigma} C_\sigma [n(\omega_\sigma)+1] g_\sigma(\omega), \qquad (1)$$

where $n(\omega_\sigma)$ is the Bose occupation factor, c is the speed of light, $g_\sigma(\omega)$ is the response function of the mode σ *normalized to one* and C_σ is the Raman coupling-to-light coefficient related to the derivative of the polarizability tensor α_σ of the mode of normal coordinate Q, $C_\sigma \propto (\partial\alpha_\sigma/\partial Q)^2$. The fluctuation–dissipation theorem relates the power spectrum to the imaginary—or dissipative—part of the susceptibility, $\chi''(\omega_\sigma)$, which is simply the Raman spectrum I_{RS} divided by the Bose factor. Considering the same incoming energy $\hbar\omega_I$ and scattering volume V_S, it is worthwhile to normalize χ'' with respect to the glass density ρ and the scattered energy:

$$\chi''_N(\omega_\sigma) = \frac{1}{\rho}\frac{1}{\omega_S^3}\frac{I^{RS}(\omega_\sigma)}{[n(\omega_\sigma)+1]}. \qquad (2)$$

Combining equations (1) and (2), the quantity to be conserved in the Raman spectra of a mode σ is thus

$$I_N^{RS}(\omega_\sigma) = \omega_\sigma \chi''_N(\omega_\sigma) \propto C_\sigma g_\sigma(\omega). \qquad (3)$$

In glasses, the description of the vibrations by normal modes failed owing to the structural disorder, and the Raman response of a given mode σ rather results in an inhomogeneously broadened line. Hence, one usually transforms ω_σ into ω in (1) and (3), and the response function $g_\sigma(\omega)$ into a Raman vibrational density of states of the mode σ [15]. In this case I_N^{RS} identifies with the so-called reduced Raman spectra defined, for example, in [16], normalized by the glass density.

The normalized parallel-polarized (VV) Raman spectra of our three silica samples, $I_N^{RS} = \omega\chi''_N(\omega)$, are reproduced in figure 1(a). This presentation completely masks the boson peak at low frequency [17, 18]. The signal is dominated by the R-band whose maximum in I^{RS} is at ∼437 cm^{-1} in v-SiO_2. This broad structure is surrounded by the relatively weak D_1 and D_2 narrow lines. The frequency of each of these three components increases with increasing density, while the reverse applies for the high frequency doublet (ω_2, ω_3) centered around 1100 cm^{-1}. This opposite behavior originates

from the different nature of the modes: bending type for the former and stretching type for the latter [3].

On the basis of these experimental data, it would be interesting to examine how C_σ and g_σ behave, depending on the nature of the vibration. Let us consider first the threefold and fourfold ring modes D_2 and D_1, associated with the breathing of the oxygen atoms [8]. It has been stated in [7] that the Raman coupling coefficient C of these bands changes upon densification, in particular owing to the puckering of the rings. The small rings being very rigid, this effect should be, however, weaker in these structures than for the network bending modes. We found in [5] that 20% densification leads to about 26% extra intensity for the R-band. This cannot account for the corresponding ∼150% and ∼400% intensity increase for the D_1 and D_2 lines, respectively, and shows that this strong intensity variation is not related to a change in the coupling factor C. There are also very few of these structures: about 1 threefold ring out of 670 SiO_2 units and 1 fourfold ring out of 550 SiO_2 units in v-SiO_2 [13]. Therefore, they can be considered as incoherent scatterers. Owing to the above two arguments, it is reasonable to assume that the Raman vibrational density of states of the small rings is proportional to their number N_σ ($\sigma = D_1$ and D_2) in the glass, that is $\int_\sigma g_\sigma(\omega)\,\mathrm{d}\omega \propto N_\sigma$. Following equation (3), the area $\mathcal{A}_\sigma$ of the D_1 and D_2 lines thus relates to the number of scatterers:

$$\mathcal{A}_\sigma(\rho) = \int_\sigma I_N^{RS}(\omega)\,\mathrm{d}\omega \propto N_\sigma(\rho). \tag{4}$$

The relatively small increase of the $n = 4$ rings up to $\rho = 2.63\ \mathrm{cm}^{-1}$ (∼1.5) suggests that the overlap of the R-band with D_1 upon densification mostly relates to a change of the Si–O–Si network angle, whose value tends to that of the $n = 4$ rings in our most densified sample, rather than to a strong increase of the number of these rings.

The Raman intensity of the network modes (R, ω_1, ω_2 and ω_3) behaves differently. The number of these vibrations remains constant upon densification, if one neglects the formation of new fifth- and sixth-coordinated Si atoms [19, 7], which indeed have never been experimentally observed, at least for 20% densification. Therefore, the total density of state for the modes $\sigma = R$, ω_1, ω_2 and ω_3 should be constant in our three glasses. However, the total integrated intensity in figure 1(a), $\int_0^{1400} I_N^{RS}(\omega)\,\mathrm{d}\omega$, increases by ∼1.17 and ∼1.24 for 10% and 20% densification, respectively. One also observes that this increase mainly concerns the bending modes, and in particular the R-band. This effect can be explained by a change in C_σ. Indeed, considering the contribution from O and Si atoms separately, numerical simulations have shown that the VV-polarized Raman spectra of the R-band (as well as for the D_1 and D_2 lines) arise almost exclusively from coupling to O-motions. For those O-bending vibrations, the intensity is related to the inter-tetrahedra Si–O–Si angle by [13]

$$C_\sigma = \alpha \cos^2(\theta_\sigma/2), \tag{5}$$

where θ_σ is the Si–O–Si angle in the mode σ and α relates to the Raman susceptibility. Coupling factors in v-SiO_2, in α-quartz and in a set of cristobalite structures calculated by first principles can be described with the same value of α [13, 20], emphasizing that α also remains the same in our densified samples. It is thus reasonable to assume that, for all but the D_1 and D_2 lines (and the boson peak), the variation of the Raman normalized area reflects changes in the coupling-to-light coefficient through

$$\mathcal{A}_\sigma(\rho) = \int_\sigma I_N^{RS}(\omega)\,\mathrm{d}\omega \propto C_\sigma(\rho). \tag{6}$$

Combining (5) and (6) it is in principle possible to extract the average Si–O–Si network angle in our densified samples provided one has a reference angle, such as, for example, that in v-SiO_2. In the literature, the value of the average Si–O–Si angle in v-SiO_2, θ_0, can vary from ∼140° to ∼155°, depending on the experiment or on the simulation. We will consider in the calculations below $\theta_0 = 144°$ obtained in a computed glass from which the Si–O–Si angles in the $n = 4$ and 3 rings have also been estimated [13]. These are smaller than in the network, $\theta_{0,D_1} \sim 136°$ and $\theta_{0,D_2} \sim 129°$, respectively.

We will show in the following that the intensity measurement provides information on the symmetry of the vibrations in silica glasses. Combining Raman intensity and frequency dependence of the bending modes in d-SiO_2, it is also possible to access the Raman coupling coefficient of the O-bending modes and the Si–O–Si angle in the network as well as in the small rings.

3. Discussion

Figure 1(b) shows the relative area, $\mathcal{A}_\sigma^{rel}(\rho) = \mathcal{A}_\sigma(\rho)/\mathcal{A}_\sigma(2.21)$, for each of the network Raman bands and the two d-SiO_2 samples. This quantity directly relates to a change in the coupling coefficient $C_\sigma^{rel}(\rho)$ of the mode σ (equation (6)) relative to that of v-SiO_2. The background underneath the three high frequency bands ($\omega_1, \omega_2, \omega_3$) has been subtracted before calculation. It is this background subtraction which gives the main contribution to the corresponding error bars in figure 1(b). For the high frequency doublet, the areas $\mathcal{A}_{\omega_2}$ and $\mathcal{A}_{\omega_3}$ result from a fit with two Gaussians, while $\mathcal{A}_{\omega_1}$ is obtained by integration of the background-corrected RS data over the ω_1 line. For the R-band, the integration runs between 100 and 700 cm^{-1}. Here, the contribution from the D_2 line has been subtracted by the procedure described in [5], but not the one from D_1 underneath the R-band. However, D_1 contributes at most to ∼2% of the signal and, as mentioned above, its intensity does not change much upon densification.

The coupling coefficient of the R-band, $C_R(\rho)$, is clearly the most affected by the compaction. In contrast, the one of ω_2 and ω_3 is lower than—or at least close to—one. The R-band corresponds mainly to bending (B) vibrations and, according to (5), its coupling coefficient should increase in d-SiO_2 owing to the decrease of the average Si–O–Si angle. This is well reproduced by the experiment. The high frequency doublet (ω_2, ω_3) rather involves a stretch (S) of the Si–O bonds [21]. It is likely that the coupling coefficient for these modes does not change much with the glass density because the tetrahedra are weakly affected by the compaction. In between, ω_1 is associated with mixed bending and stretching

motions [21] (B+S) and its coupling coefficient thus exhibits an intermediate behavior. Therefore, the trend of C_σ with density qualitatively reflects the bending or stretching nature of the modes. It is likely that such a behavior generalizes to elastically compressed (e.g. in a diamond anvil cell) silica glasses, but also to other network glasses such as GeO_2, GeS_2, $GeSe_2$ and B_2O_3.

Let us discuss now the frequency dependence of the bending modes. Using a nearest-neighbor central-force model, Sen and Thorpe [3] have proposed earlier the relation $\omega = \sqrt{\beta/m}\cos\theta/2$, where β is a restoring force constant and m an effective mass for the vibrating structures. The latter simply corresponds to the oxygen mass in an Si–O–Si motion where the Si atoms are fixed. To go further in our analysis we first need to make two approximations. The first one is to consider that β is constant whatever the glass density. This is probably a more reasonable approximation for the small rings (D_1 and D_2) than for the larger structures (R-band), because the denser the structure the weaker the effect on compaction. The second approximation assumes that the Sen and Thorpe expression above remains valid for the breathing of small rings, although these vibrations involve a slight stretching of the Si–O bond and are thus not pure bending motions. However, we will further demonstrate that the Raman analysis of the Si–O–Si angles in rings is in very good agreement with the computed literature data, suggesting that the above two assumptions are reasonable. Assuming β is constant, one thus has

$$\cos\theta/2 = \frac{\cos\theta_0/2}{\omega_0}\omega, \tag{7}$$

where ω_0 and θ_0 is a reference set of data. Taking $\omega_0 = \omega_R = 437\ cm^{-1}$ at the maximum of the R-band in I^{RS}, one has $\cos\theta/2 = 7.071 \times 10^{-4}\omega$. We applied this formula in v-SiO_2 at frequencies corresponding to D_1 and D_2, $\omega = \omega_{D_1} = 495\ cm^{-1}$ [5] and $\omega = \omega_{D_2} = 605\ cm^{-1}$, to see whether this relation could remain valid for the breathing modes of small rings. Surprisingly we find $\theta_{D_1} = 139.0°$ and $\theta_{D_2} = 129.3°$, which compares rather well with $\theta_{0,D_1} \sim 136°$ and $\theta_{0,D_2} \sim 128°$ proposed by the simulations [13]. It is worth noting here that θ_0, θ_{0,D_1} and θ_{0,D_2} have been obtained from the same model glass. θ_0 being the reference value in our calculations, this prevents us from large uncertainties when comparing experiment and simulation data.

The departure between experiment and calculation could eventually be explained by the nature of the breathing modes D_1 and D_2 which are not pure bending vibrations as they involve a slight stretching of the Si–O bonds. However, the dominant effect probably arises from the Raman coupling factor of the O-bending modes, $C_B(\omega)$, which shifts the peak maximum in the Raman spectra. Combining (5) and (7) one finds $C_B(\omega) \propto \omega^2$. The quantity $I_N^{RS}/C_B(\omega)$ presented in the inset of figure 1(a) thus corresponds to the Raman density of state $g_B(\omega)$ (equation (3)) of the bending modes. The experimental value for the area of $g_B(\omega)$ is constant in our three glasses with an accuracy better than 5%, emphasizing the self-consistency of our approach. The normalization of the Raman spectra by $C_B(\omega)$ decreases by about 3 the signal at high frequency (the inset of figure 1(b)), in particular in the frequency region of D_1 and D_2. Such a presentation gives a more appropriate view of the weight of these modes relative to the R-band and likely explains the difficulty of observing the breathing modes of small rings in the full vibrational density of states measured by neutron scattering [22]. At low frequency, $g_B(\omega)$ artificially increases owing to the proximity of the boson peak, whose weight is magnified by the normalization by $C_B(\omega)$. In v-SiO_2, the maximum of the R-band in a $g_B(\omega)$ plot is now $\omega_R = \omega_0 = 422\ cm^{-1}$ and equation (7) becomes $\cos\theta/2 = 7.323 \times 10^{-4}\omega$. Table 1 summarizes the values of θ_σ and $\Delta\theta_\sigma$ extracted from this refined formula.

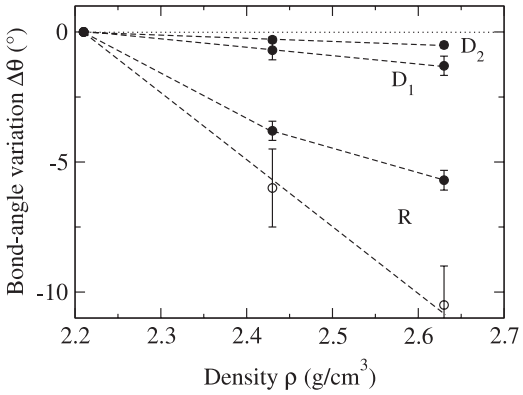

Figure 2. Si–O–Si bond angle reduction in the network (R) and in the small rings (D_1 and D_2). For the highly dissymmetric R-band it is useful to consider both the shift of the maximum of the distribution (●) and that of the center of gravity (○) of the distribution.

ω_σ is the frequency at the peak maximum for the R-(network), D_1- ($n = 4$ rings) and D_2-band ($n = 3$ rings). Therefore, θ_R corresponds to the angle at the maximum of the distribution that is, the most probable network angle. It likely corresponds to the average angle in the structures with $n \simeq 6$, which are the most probable ones [4]. In v-SiO_2 the Si–O–Si angle in the $n = 4$ and 3 rings obtained from our Raman-spectra analysis, 137.9° and 127.6° respectively, are now very close to the calculated ones (∼136° and ∼128°). This shows that (7) gives a reasonable estimate of the Si–O–Si angle for all the O-bending vibrations, *including those in small rings*. Therefore, for frequencies between ∼200 and ∼700 cm^{-1} it is possible to draw an x axis showing the angles rather than the frequency (inset of figure 1(a)). For frequencies below ∼200 cm^{-1}, one cannot exclude the scattering from more collective motions.

$\Delta\theta_\sigma = \theta_\sigma(\rho) - \theta_\sigma(2.21)$ is the variation of θ_σ (σ = R, D_1, D_2) in the two densified glasses, relative to v-SiO_2. The glass-density dependence of $\Delta\theta_\sigma$ is presented in figure 2. The reduction of the most probable network angle seems to saturate at high densities. One finds $\Delta\theta_R = -5.7°$ for 20% densification. Using magic angle spinning nuclear magnetic resonance (MAS-NMR) on the ^{29}Si nucleus, Devine *et al* [23] found a variation of ∼−5° for a 16%-densified sample compacted at 50 kbar and 600 °C. A linear glass-density dependence would lead to a shift of −6.2°, a value in very good agreement with our result, considering that such a linear extrapolation gives a slightly overestimated value (see figure 2). The effect of compaction on the Si–O–Si bond angle decreases in the denser structures. For 20% densification it

Table 1. Si–O–Si angles in our three silicas, θ_R, θ_{D_1} and θ_{D_2}, calculated from their Raman spectra. The related frequencies ω_R, ω_{D_1} and ω_{D_2} correspond to the peak maxima in a $g_B(\omega)$ plot. The values in parentheses, obtained from the raw Raman spectra (I^{RS}) are given for comparison. $\Delta\theta$ is the angle in d-SiO_2 relative to that in v-SiO_2 (see text). For the dissymmetric R-band one distinguishes two quantities: the shift of the peak maximum, $\Delta\theta_R$, and the shift of the center of gravity of the distribution, $\Delta\theta_R^G$. $\delta\theta_R$ is the full width at half-maximum of the distribution. Frequencies are in cm^{-1}.

	Network (R)					$n = 4$ rings (D_1)			$n = 3$ rings (D_2)		
Density ρ (g cm^{-3})	ω_R	θ_R	$\Delta\theta_R$	$\Delta\theta_R^G$	$\delta\theta_R$	ω_{D_1}	θ_{D_1}	$\Delta\theta_{D_1}$	ω_{D_2}	θ_{D_2}	$\Delta\theta_{D_2}$
2.21	422 (437)	144[a]	—	—	32	490 (495)[b]	137.9	—	603 (605)	127.6	—
2.43	465 (468)	140.2	−3.8	−6	20	498 (506)[b]	137.2	−0.7	606 (609)	127.3	−0.3
2.63	486 (493)	138.3	−5.7	−10.5	16	505 (515)[b]	136.6	−1.3	608.5 (614)	127.1	−0.5

[a] From computer simulation [13].
[b] From ISRS measurements [5].

goes from $\Delta\theta = -5.7°$ in structures with $n \simeq 6$, to $-1.3°$ in the fourfold rings ($n = 4$) and $-0.5°$ in the threefold ones ($n = 3$). These numbers confirm that the small rings are only weakly affected by the densification.

It is also useful to estimate the shift of the center of gravity of the network angle distribution in the densified glasses, as it is sometime done in the simulations. This requires us to define the frequency at the center of gravity of the R-band in (7):

$$\omega^G = \frac{\int \omega g_B(\omega)\, d\omega}{\int g_B(\omega)\, d\omega}. \quad (8)$$

The dissymmetry of the R-band associated with the signal arising from the boson peak at low frequency complicates the calculation of ω^G. In order to minimize the relative errors, the integration is done between $\omega_R - \Gamma/2$ and $\omega_R + \Gamma/2$, where Γ is the full width at half-maximum of the distribution. One calculates $\omega_R^G(2.21) \simeq 357$ cm^{-1}, $\omega_R^G(2.43) \simeq 413$ cm^{-1} and $\omega_R^G(2.63) \simeq 463$ cm^{-1}. This corresponds to an angle reduction $\Delta\theta_R^G = -6° \pm 1.5°$ and $\Delta\theta_R^G = -10.5° \pm 1.5°$ for 10% and 20% densification, respectively. The large error bars for the angle variation account for the choice of the integration limits in (8). Though the value for the glass with highest density compares rather well to that obtained from recent numerical simulations $\Delta\theta^G \sim -8°$ [24]. It is also about twice the value found above for the shift of the maximum of the distribution ($-5.7°$), a difference which can easily be understood by a faster decrease of the volume fraction of the open structures (large angles, low frequencies) in the first step of the densification.

Looking to the shape of $g_B(\omega)$ one also notices the large spread of the Si–O–Si angles. In v-SiO_2 one can tentatively estimate a full width at half-maximum $\delta\theta \simeq 32°$. The angular spread decreases in the densified samples. One has $\delta\theta \simeq 20°$ for $\rho = 2.43$ g cm^{-3} and $\delta\theta \simeq 16°$ for $\rho = 2.63$ g cm^{-3}. The stiff decrease of $g_B(\omega)$ at high frequency certainly arises from a close-packing-type effect of the SiO_4 tetrahedra which limits the angular spread at low angles. This could also explain the saturation of $\delta\theta$ when increasing the glass density.

Finally it is important to notice that the local structure of the densified silicas can change depending on the densification process. This is clearly observed when comparing glasses compacted by shockwave and by hydrostatic pressure at high temperature [25]. Computed densified silicas in [7, 24] have been obtained by an instantaneous reduction of the sample volume at room temperature, followed by a relaxation (between 2 and ∼8 ps, depending on the model glass) of the structure. This densification process is also very different from that employed to obtain our samples. This points out that a comparison of the fine structure of d-SiO_2 glasses obtained with a different pressure–temperature cycle should be taken very cautiously.

4. Conclusion

Intensity and frequency analysis of the Raman spectral lines of permanently densified vitreous silicas have been performed. The Raman coupling coefficient C is sensitive to the bending or stretching character of the modes. For the O-bending vibrations, one has $C_B(\omega) \propto \omega^2$. The frequency dependence of these modes, including those in small rings, can reasonably be described by a single law which only takes into account the Si–O–Si angle, provided the Raman spectra are normalized by C_B. This suggests that for Raman modes between 200 and 700 cm^{-1} typically, the frequency of the vibrations is determined by one single Si–O–Si structural unit, whatever the number of these structures vibrating with a phase relationship. For 20% densification we find a reduction of ∼1.3° and ∼0.5° in the fourfold and threefold rings, respectively. These values are very small, confirming that the small rings only weakly pucker upon compression. This also supports [5] that the normalized Raman intensity of the D_1 and D_2 spectral lines is proportional to the number of rings. In our most densified sample, the maximum of the network bond angle distribution shifts by ∼5.7° while it is rather ∼10.5° if one considers the center of gravity of the distribution. The former value is very close to that extrapolated from previous NMR studies in a sample densified with a similar pressure–temperature cycle than ours. As both the Si–O–Si bond angle distribution and the small ring statistics likely depend on the densification cycle, this simple Raman-spectra analysis could become part of the routine characterization of the local and medium range structure of permanently densified silicas, elastically compressed glasses [26] and nanoindented surfaces [27]. To

some extent it could also be applied to other silica-based glasses.

Acknowledgment

The author thanks M Arai for providing the high quality densified samples.

References

[1] Trachenko K, Dove M T, Hammonds K, Harris M J and Heine V 1998 *Phys. Rev. Lett.* **81** 3431
[2] Giddy A P, Dove M T, Pawley G S and Heine V 1993 *Acta Crystallogr.* A **49** 697
[3] Sen P N and Thorpe M F 1977 *Phys. Rev.* B **15** 4030
[4] Giacomazzi L, Umari P and Pasquarello A 2009 *Phys. Rev.* B **79** 064202
[5] Burgin J, Guillon C, Langot P, Vallée F, Hehlen B and Foret M 2008 *Phys. Rev.* B **78** 184203
[6] Inamura Y, Arai M, Nakamura M, Otomo T, Kitamura N, Bennington S M, Hannon A C and Buchenau U 2001 *J. Non-Cryst. Solids* **293–295** 389
[7] Rahmani A, Benoit M and Benoit C 2003 *Phys. Rev.* B **68** 184202
[8] Galeener F L 1982 *Solid State Commun.* **44** 1037
Galeener F L 1982 *J. Non-Cryst. Solids* **49** 53
[9] Galeener F L and Mikkelsen J C Jr 1981 *Phys. Rev.* B **23** 5527
[10] Pasquarello A and Car R 1998 *Phys. Rev. Lett.* **80** 5145
[11] Galeener F L and Geissberger A E 1983 *Phys. Rev.* B **27** 6199
[12] Polsky C H, Smith K H and Wolf G H 1999 *J. Non-Cryst. Solids* **248** 159
[13] Umari P, Gonze X and Pasquarello A 2003 *Phys. Rev. Lett.* **90** 27401
[14] Hayes W and Loudon R 2004 *Scattering of Light by Crystals* (Mineola, NY: Dover)
[15] Shuker R and Gammon R W 1970 *Phys. Rev. Lett.* **25** 222
[16] Galeener F L, Leadbetter A J and Stringfellow M W 1983 *Phys. Rev.* B **27** 1052
[17] Hehlen B, Courtens E, Vacher R, Yamanaka A, Kataoka M and Inoue K 2000 *Phys. Rev. Lett.* **84** 5355
[18] Hehlen B, Courtens E, Yamanaka A and Inoue K 2002 *J. Non-Cryst. Solids* **307** 87
[19] Susman S, Volin K J, Price D L, Grimsditch M, Rino J P, Kalia R K, Vashishta P, Gwanmesia G, Wang Y and Liebermann R C 1990 *Phys. Rev.* B **43** 1194
[20] Umari P, Pasquarello A and Del Corso A 2001 *Phys. Rev.* B **63** 094305
[21] Taraskin S N and Elliott S R 1997 *Phys. Rev.* B **56** 8605
[22] Carpenter J M and Price D L 1985 *Phys. Rev. Lett.* **54** 441
[23] Devine R A B, Dupree R, Farnan I and Capponi J J 1987 *Phys. Rev.* B **35** 2560
[24] Matsubara M, Ispas S and Kob W 2009 private communication
[25] Sugiura H, Ikeda R, Kondo K and Yamadaya T 1997 *J. Appl. Phys.* **81** 1651
[26] Champagnon B, Martinet C, Boudeulle M, Vouagner D, Coussa C, Deschamps T and Grosvalet L 2008 *J. Non-Cryst. Solids* **354** 569
[27] Perriot A, Vandembroucq D, Barthel E, Martinez V, Grosvalet L, Martinet C and Champagnon B 2006 *J. Am. Ceram. Soc.* **89** 596